Video Article

A Full Skin Defect Model to Evaluate Vascularization of Biomaterials *In Vivo*

Thilo L. Schenck[1], Myra N. Chávez[1], Alexandru P. Condurache[2], Ursula Hopfner[1], Farid Rezaeian[3], Hans-Günther Machens[1], José T. Egaña[1,4]

[1]Department of Plastic Surgery and Hand Surgery, University Hospital rechts der Isar, Technische Universität München

[2]Institute for Signal Processing, University of Lübeck

[3]Department of Plastic Surgery and Hand Surgery, University Hospital Zürich

[4]FONDAP Center for Genome Regulation, Facultad de Ciencias, Universidad de Chile

Correspondence to: José T. Egaña at tomasega@gmail.com

Abstract

Insufficient vascularization is considered to be one of the main factors limiting the clinical success of tissue-engineered constructs. In order to evaluate new strategies that aim at improving vascularization, reliable methods are required to make the in-growth of new blood vessels into bio-artificial scaffolds visible and quantify the results. Over the past couple of years, our group has introduced a full skin defect model that enables the direct visualization of blood vessels by transillumination and provides the possibility of quantification through digital segmentation. In this model, one surgically creates full skin defects in the back of mice and replaces them with the material tested. Molecules or cells of interest can also be incorporated in such materials to study their potential effect. After an observation time of one's own choice, materials are explanted for evaluation. Bilateral wounds provide the possibility of making internal comparisons that minimize artifacts among individuals as well as of decreasing the number of animals needed for the study. In comparison to other approaches, our method offers a simple, reliable and cost effective analysis. We have implemented this model as a routine tool to perform high-resolution screening when testing vascularization of different biomaterials and bio-activation approaches.

Video Link

The video component of this article can be found at http://www.jove.com/video/51428/

Introduction

In the recent decades, tissue engineering has opened up a new therapeutic option to replace tissue defects with the body's own cells[1]. In order to support the physiological process of tissue regeneration, scaffolds are designed as a biodegradable structure, that provides a scenario where cells from the wound bed can grow and restore the defect[2,3].

Insufficient vascularization is considered to be the main obstacle, which holds back the clinical breakthrough of bioartificial scaffolds[4]. With the ingrowth of cells, the demand for nutrients and oxygen increases and vascularization of the material becomes essential. Insufficient or delayed vascularization can therefore lead to central necrosis of tissue-engineered products[5]. In addition, blood vessels provide immune competent cells and remove the metabolic residues in the regenerating area. High infection rates and low regeneration are only some of the consequences of insufficient blood perfusion observed in tissue engineering, which are aimed to be averted by increasing the vascularization of the scaffolds[6,7].

Several strategies that aim at improving vascularization focus on the key role of the biomaterial itself and the microstructure of the scaffold. There are intensive research efforts to develop new approaches in shifting the healing process from *repair* to *regeneration*, thereby (re)generating a tissue with the closest physiological properties to the one to be restored[8,9]. Biomaterials that were studied and evaluated with regards to their regenerative potential included collagen, fibrin, chitosan and alginate[10,11]. These biomaterials can be used and combined as a backbone for building new scaffolds using different strategies such as tissue decellularization, self-assembly, rapid prototyping and electrospinning[12]. In order to enhance the body's own regenerative capacity, scaffolds can be bioactivated. The incorporation of recombinant angiogenic growth factors[13] or gene vectors encoding for such factors[14] has shown to improve vascularization of the scaffold. The use of stem cells has been widely shown to be a promising strategy to improve vascularization, where mesenchymal stromal cells and endothelial progenitor cells have gained the most attention[15,16]. Other approaches attempt to build constructs that contain prefabricated vessel networks prior to transplantation[17]. Despite intensive efforts in scaffold design and their bio-activation, no strategy has improved vascularization at a clinically significant level and, with the exception of dermal replacements in massive burn injuries, the translation of bioengineered materials into the clinical routine is only taking place hesitantly[18].

One of the reasons why vascularization of artificial tissue constructs is still an unsolved problem, is the difficulty to evaluate the success of new technologies in *in vivo* approaches. Although *in vitro* experiments may provide important insights of the vascularization potential of scaffolds, appropriate animal models are required to study key parameters such as the biocompatibility of the material, the safety and efficacy of the

treatment and, of particular importance, the vascularization of the tissue construct. Therefore, reliable tools to visualize and quantify blood vessel networks *in vivo* are essential.

In this study we present a simple and reliable method that allows the visualization and quantification of the vascular network inside explanted scaffolds. This method is based on tissue transillumination and digital segmentation. Since this method is non-invasive, it allows further molecular and histological analyses of the target material.

Protocol

1. Preparation of Scaffolds

1. Generate samples of the scaffolds by using 12 mm biopsy punches.
2. To introduce bioactive molecules or cells into the scaffold, drain the scaffolds by gently squeezing them with a sterile gauze. Then rehydrate the scaffolds by adding 160 µl of a solution containing the bioactive molecules or cells of interest. Double-check the success of bioactivation with cells through metabolic assays such as MTT Assays.
3. If necessary, fix the compounds or cells to be tested inside the scaffold by delivering them, for instance in a fibrin-thrombin solution or a hydrogel, again through rehydration as described in step 1.2.
    NOTE: This step can be of helpful when compounds or cells do not mechanically attach to the material. One can also control the release dynamics of the compounds..
4. Prepare the titanized meshes, which will be placed under each scaffold in every experiment and control group, by cutting out round shaped pieces, approximately 14 mm in diameter.
    NOTE: The titanized mesh works as a physical border required to delimit the regenerated tissue from the wound bed.

2. Animals

1. Prior to implementation of the presented model, consult the corresponding animal protection laws and obtain permission from the local authorities. In this work, all experiments were performed with mice, according to the current German animal welfare act and approved by the District Government of Upper Bavaria (Regierung von Oberbayern).
2. Carefully choose the animal and strain. Although the model was established for mice, it can be translated to other common animals, such as rats, rabbits or pigs.
3. In case you are working with furred animals, shave the back of the animals before implantation of the scaffolds.
    NOTE: This work uses mice of 6 to 8 weeks of age with a body weight between 20 g and 25 g, however different ages and body weights can also be used.

3. Anesthesia

1. Conduct the operation under sterile conditions. In order to maintain the animal's normal body temperature, use a warming mat.
2. Prior to inhalative anesthesia the animals receive Buprenorphin at a dose of 0.05-0.1 mg/kg bodyweight, subcutaneously every 8 hr.
3. Place the animal under inhalative anesthesia (Isoflurane) or apply equivalent standard procedures. Confirm anesthesia either by gently squeezing the animal's toes or through a skin pinch.
4. To prevent exsiccosis, inject 0.5 ml physiologic saline solution subcutaneously at the beginning of the operation.

4. Excision of the Skin

1. Place the animal in a prone position and mark the midline of the mouse's back with a fine tip permanent pen (**Figure 1A**).
2. Define the excision area. Place the defects in the area shown in **Figure 1C**. Note that if the defects are placed too caudally, animals are more prone to remove the dressings and the scaffolds.
3. Create round bilateral defects using a 10 mm biopsy punch (**Figure 1B**). The punch should be carefully forced against the skin and must not be used to cut completely through the skin, but to delineate the excision area (**Figures 1C & 1E**).
4. Gently lift off the marked skin with forceps and incise along the marked circle using fine surgical scissors (**Figure 1F**). In case of bleeding, carefully compress with sterile gauze. A step-by-step description of the excision is shown in **Figure 1**.
    NOTE: The defect is created with a smaller punch than the one for generating the scaffolds, to compensate the enlargement of the defect due to the skin elasticity.

5. Scaffold Implantation

1. In order to make space for the titanized mesh, extend the separation of skin and underlying tissue at the wound borders for 2-4 mm (**Figure 2A**).
2. Place the titanized mesh into the defect directly on the wound bed and under the wound edges (**Figures 2A & B**).
3. Place scaffolds directly over the mesh.
4. Suture the scaffolds to the adjacent wound edges with 4 to 6 single knots, leaving the edges slightly over the scaffold (**Figure 2C**).
    NOTE: Avoid the use of biodegradable sutures.
5. Suture a transparent wound dressing above the defects to protect the scaffold while allowing monitoring of the wound area (**Figure 2D**).

6. Postoperative Care

1. Keep one mouse per cage to avert mutual manipulation of the dressing and scaffolds.
2. Evaluate the general state of the animal on a daily basis by observing motor activity, body weight, signs of pain, tolerance to the dressing and auto-mutilation. Also monitor the wound area for bleeding, local and systemic signs of infection and the position of the dressing.
3. In order to minimize the pain of the animal, inject Buprenorphin daily at a dose of 0.05-0.1 mg/kg bodyweight or equivalent analgesic medication.
4. If the mouse removes or damages the wound dressing, replace or reattach it under anesthesia.

# 7. Euthanasia and Explantation of the Scaffold

1. At desired time points, sacrifice the animals by overdoses of Pentobarbital (150 mg/kg).
2. Mark the site of skin excision with a permanent marker, which should include the scaffolds and as much of the mouse back skin as possible (**Figure 3A**).
3. Incise the skin along the marked lines with a pair of scissors or a scalpel. Detach the entire skin, including the scaffolds and the titanized mesh, from the underlying tissue through blunt preparation (**Figure 3B**).
4. Place the explanted tissue stretched out on a Petri dish (**Figure 3C** and **D**)

8. Visualization and Quantification of the Vascular Network

1. Transillumination:
   1. Set up a transillumination device, by mounting a Petri dish above a strong source of white light (100 Watt standard light bulb).
   2. Fix a digital camera above the transilluminator to obtain digital pictures.
   3. Place the samples upside down on the Petri dish over the transillumination device.
   4. Take pictures of the complete scaffolds in macro mode as well as of equally sized areas of normal skin. Store the images in a TIFF format for further digital analysis.
   5. Save the tissue for further biochemical or histological analysis.

2. Digital segmentation and quantification:
   1. Download and install the VesSeg-Tool software, which can be obtained free of charge at: http://www.isip.uni-luebeck.de/index.php?id=150&L=2%255.
   2. Open the picture with the VesSeg-Tool software.
   3. Select the area of the image covered by the scaffold for digital analysis (Image→Select).
   4. To increase the contrast of vessels use the option "Hysteresis thresholding" (Image→Vessel enhancement filter→Hysteresis thresholding→Top-Hat transformation→Calculate vessel enhancement).
   5. Proceed with the segmentation of the vessel map (Image→Vessel enhancement filter→Hysteresis thresholding→Threshold borders). Select the first threshold ("Vessel coverage"), so every pixel, which is even remotely vessel-like, will be labeled as vessel. Select the second threshold ("Background coverage"), so only those pixels that are particularly vessel-like will be labeled as vessels.
   6. Check the automatic segmentation proposal manually to add non-captured vessels and to eliminate common false-positive structures, which usually are long and thin, vessel-like structures such as hairs or sutures.
   7. Calculate the length of the vessels and the overall area covered by vessels (Image→Image statistics→Binary image statistics). NOTE: For the calculation of the vessel-lengths, vessels in the resulting vessel map are thinned to lines with a width of one pixel[20].

3. Analyze the native skin area under the same parameters as the scaffolds, assigning a value of 100% to the native tissue and relate the scaffold to that value. For instance, if the percentage of white pixels is 60% in the normal tissue and 30% in the scaffold, it would represent a 50% vascularization of the scaffold. Note: The white vessels coverage is assigned to the area of a square around the scaffold. Adjust the number of white pixels coverage considering that the area of the circle is significantly smaller ($\pi \times R^2$) than the square ($4 \times R^2$).

Representative Results

A reliable bilateral full skin defect can be created in the mouse (**Figure 1**) where the skin can be replaced by a biomaterial under study (**Figure 2**). Here, no major complications are observed during or after the operative procedure, neither macroscopic signs of infection or foreign body reaction. In rare cases, a scaffold gets lost when a mouse removes it. Wound contraction was never observed (**Figure 3**). Tissue transillumination allowed clear visualization of vascular structures of up to 30 µm in width, in a whole tissue sample that included both, native tissue and implanted scaffolds (**Figure 4**). After digital segmentation, vessels could be easily quantified at desired times post implantation. For instance, 2 weeks after implantation, vascularization levels of 62.28 ± 8.6% were observed (mean ± standard error of mean; n=8)[21]. Altogether, about 25 min per animal (2 scaffolds) are required for the implantation, 5 min for tissue harvesting and picturing and 10 min for digital analysis of one sample. As a final point, this method does not affect the quality of the explanted tissue for further analysis. For instance, proteins and RNA extracts can be easily obtained from the sample by standard methods.
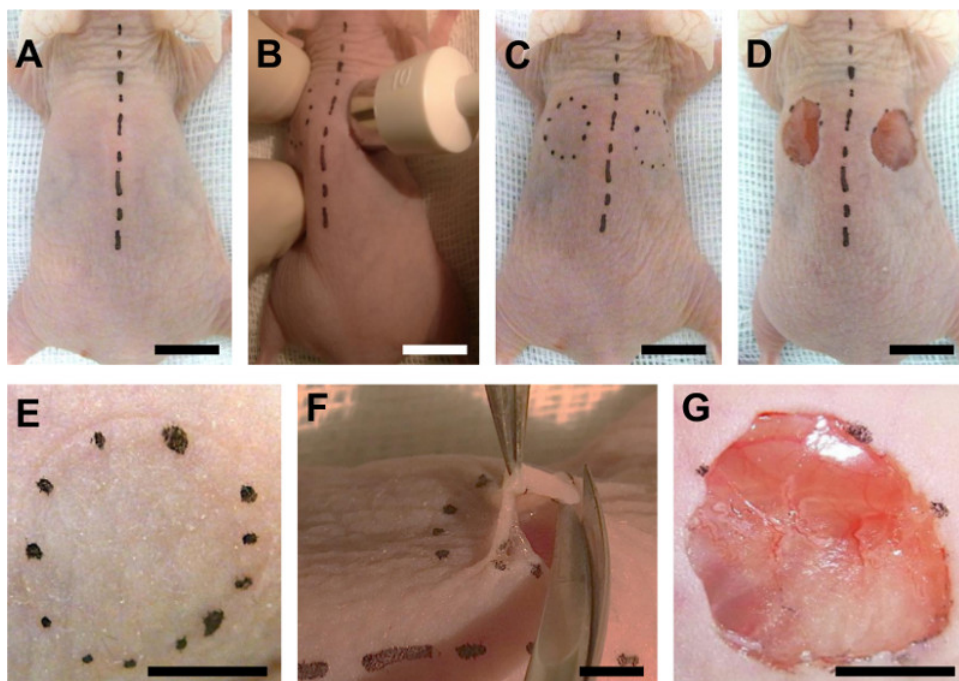
Figure 1. Full Skin Defect. The midline of the mouse's back is marked with a fine tip pen and a biopsy punch is used to mark the area were the defect will be created (**A**, **B**, **C** and **D**). Once the areas are defined, full skin is removed with standard surgical scissors as seen in the close-up of the preparation (**E** and **F**). A final result of the defect is shown in (**D**) and magnified in (**G**). Scale bars represent 1 cm in ABCD and 5 mm in EFG. Please click here to view a larger version of this figure.
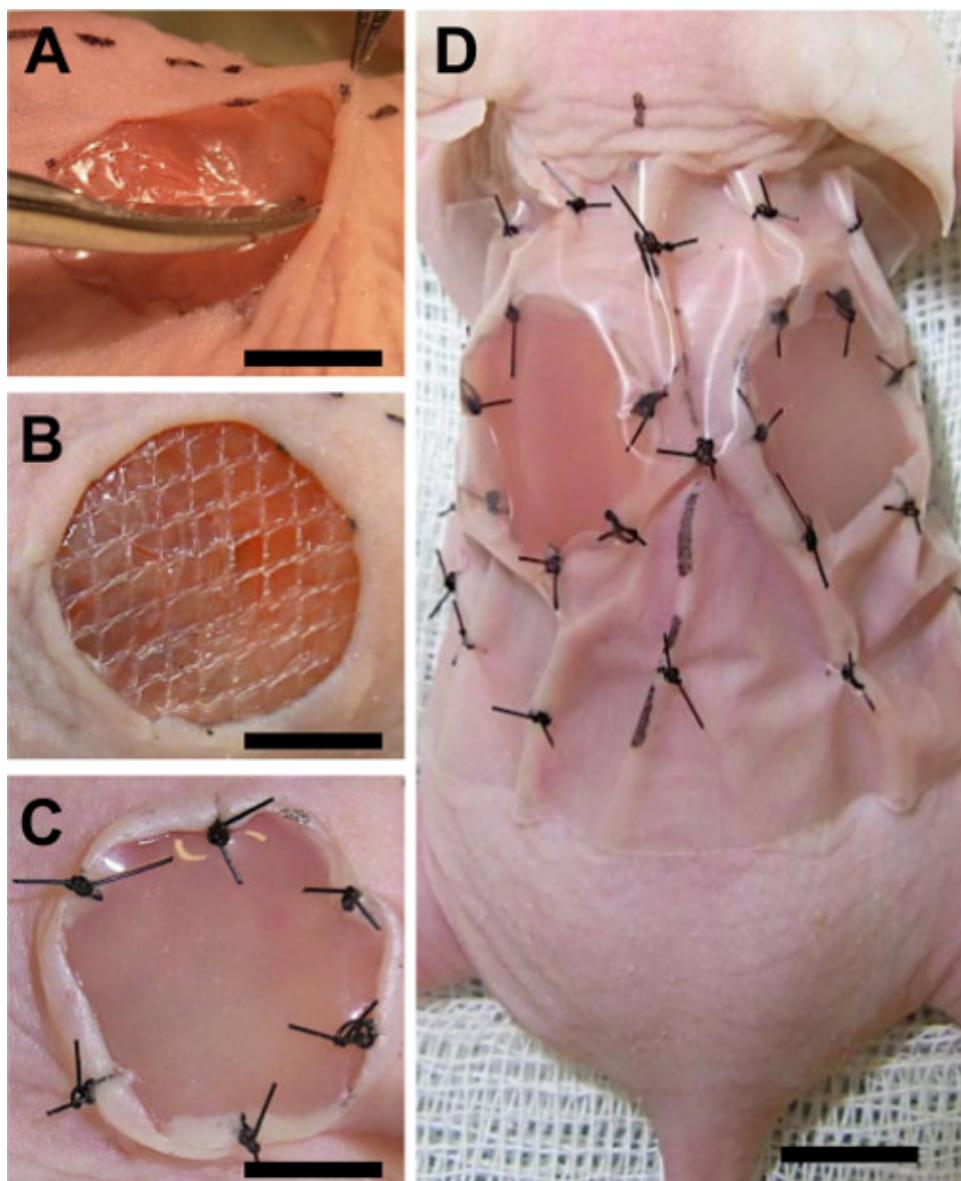
Figure 2. Implantation of the scaffold. Prior to the implantation of the scaffold, a mesh is placed into the defect directly on the wound bed and under the wound edges (**A** and **B**). Next scaffolds are placed over the mesh and sutured to the wound edges (**C**). Finally, a transparent wound dressing is placed and sutured to the skin (**D**). Scale bar represents 5 mm in (**A**, **B**, and **C**) and 1 cm in (**D**). Please click here to view a larger version of this figure.
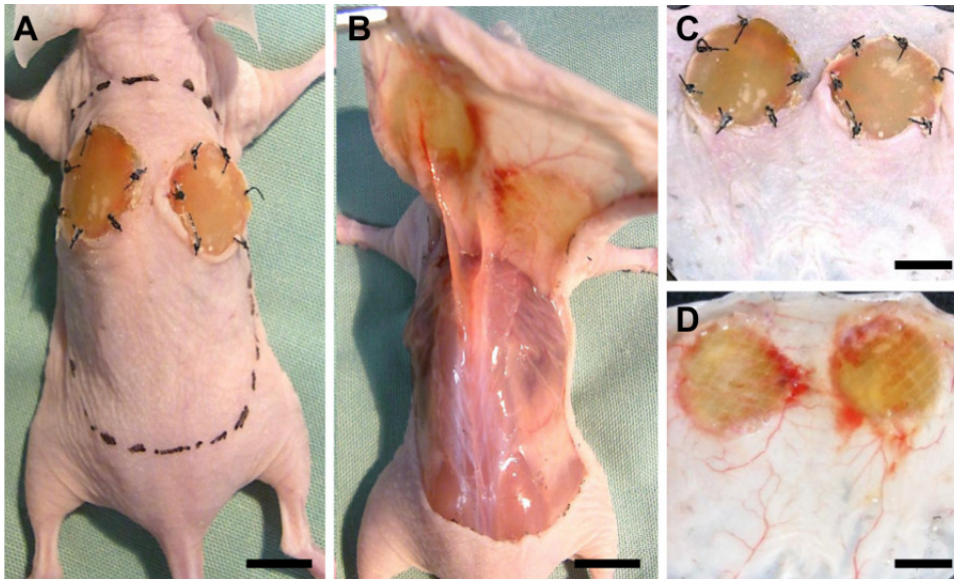
Figure 3. Tissue explantation. For tissue analysis the full skin from the back of the animal is surgically removed (**A** and **B**) and stretched out on a Petri dish (**C**). For transillumination the skin is turned upside down and a digital picture is taken (**D**). Removal of the skin next to the scaffolds is necessary for normalization of the vascularization data. Scale bars represent 1 cm. Please click here to view a larger version of this figure.
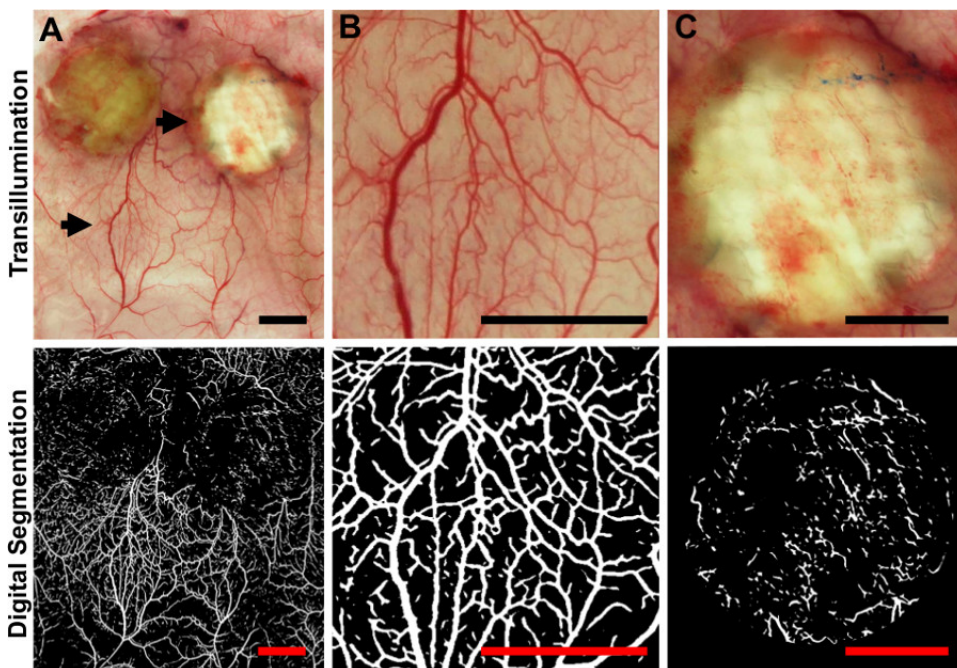
Figure 4. Transillumination, digital segmentation and quantification. Skin tissue was excised and the vascular network within was visualized by transillumination (upper pictures) Full skin of the back (**A**) and detailed areas of the native skin (**B**) and the scaffold (**C**) are shown. Arrows show the magnified areas in (**B**) and (**C**). Each of the lower pictures shows the results of the digital segmentation process for the picture located directly above. Scale bars represent 5 mm. Please click here to view a larger version of this figure.

Discussion

There is a need to establish successful approaches in improving blood perfusion in tissue engineered constructs, which demands the development of new reliable methods to study the vascularization processes within the biomaterials. Common methods for making scaffold vascularization *ex vivo* visible include the use of microscopy, which provides a high-resolution tool. In most cases, though, this method is limited to the analysis of small tissue areas and tends to be expensive and time consuming. Moreover, it often includes elaborate labeling and staining methods, where blood perfused vessels cannot be distinguished from non-functional ones[22]. Methods in use to assess the functionality of vessels are computer tomography, magnetic resonance imaging and positron electron tomography. These methods have the drawbacks of extremely costly equipment and low-resolution power[23]. Another commonly used strategy to visualize vascularization is the use of vascular casts followed by chemical corrosion of the tissue[24]. This method makes it possible to obtain a representative 3D structure of the vascular network, but the results strongly vary depending on the level of artificial perfusion and tissues cannot be used for further biochemical studies, such as

protein or RNA analysis. The chicken chorioallantoic membrane (CAM) model[25] and the skinfold chamber model in rodents[26,27] have shown to be effective methods to analyze angiogenesis, capillary perfusion and blood flow. Recently, the skinfold chamber model has also been used for tissue engineering applications evaluating MSC-based vascularization strategies in porous polyurethane scaffolds[28]. These methods present important advantages for *in vivo* imaging and represent an attractive target for the method described here.

The model presented here was developed to overcome the shortcomings of the methods mentioned above. Taking advantage of the unique intrinsic characteristics of the skin, full defects are created and used to evaluate vascularization of biomaterials. Skin is an external organ, which allows easier visualization and manipulation of the tissue. Because of its large surface and homogeneous structure, multiple defects can be created which make internal comparisons possible, while decreasing the number of animals required for the study. Due to the antero-posterior symmetry of the animal, bilateral defects are suggested, however; the influence of systemic effects should be considered when both sides are compared to each other. Finally, skin is a fairly transparent tissue representing an optimal organ of choice for transillumination. Although the method described here is suited for many different native tissues and several biomaterials, this protocol was originally established to be used with a double-layer collagen-based scaffold that is FDA-approved and clinically used for dermal repair. An important prerequisite for the implementation of this method is that the scaffold has to be partially transparent. Depending on the chosen scaffold material, some adaptation of the protocol might be required. Previously, our group has used the model to show how the application of human mesenchymal cells to scaffolds enhances their vascularization[29].

A standard digital camera and a light source are sufficient for the visualization of the vascular network, which can be quantified through free software. The semiautomatic segmentation of the pictures by the VesSeg-Tool consists of two steps. In the first step, the image taken from the vascular network is contrast-enhanced leading to a vessel map. Then, the segmentation algorithm selects the vessel areas and finally, the segmentation proposal is presented as an image (**Figure 4**)[30]. In a second processing step, using the fact that vessels are connected structures (meaning that vessel pixels hang together spatially), a second segmentation is used to select from the first one only the true vessel pixels and all true vessel pixels. Therefore, a final label of "one" is awarded only to those low-confidence vessel pixels from the first image that are connected over a chain of neighbors to a high-confidence vessel pixel in the second image.

Since no chemical additives are necessary, this method is also cost-effective. Digital analysis shows a good reproducibility at determining vessel dimensions, intravascular distances, number of branching points, vascularized area and total length of vascular network. We have previously shown that the blood vessel network can be better visualized by transillumination than through radio-angiographic studies[31]. The presence of the titan mesh has a double function. On the one hand, it prevents wound contraction, which is a common drawback of the use of mouse models; on the other hand, it provides a physical border between the scaffold and the wound bed. Because most scaffolds are biodegradable, the last-mentioned function is critical to physically delimitate the border between the scaffold and the wound bed during the harvesting of the scaffolds. Among the main drawbacks of this method is the need of explanting the scaffolds and therefore the restrain of the analysis to one single time point; thus the dynamic observation of vascularization is not possible with the current setting. Another problem is that this method is limited to semi-transparent biomaterials that permit transillumination. Finally, even though the operation procedure does not require special surgical skills, a learning curve of about 6 – 12 operated animals have to be considered to master the method properly.

We introduce a time and cost effective approach that allows high-resolution visualization and quantification of vascular structures, representing an ideal method to compare vascularization in different biomaterials or different scaffold-bioactivation strategies. This method is easy to establish and does not require special equipment. A key feature of this model is that after vessel visualization, tissues can be further used for studies such as histological or molecular analysis.

Disclosures

Conflict of interest statement:

All authors: None

Financial Disclosures:

None of the authors has a financial interest in any of the products, devices, or drugs mentioned in this manuscript.

Acknowledgements

References

1. Rahaman, M.N., Mao, J.J. Stem cell-based composite tissue constructs for regenerative medicine. *Biotechnology and Bioengineering.* **91** (3), 261-284, doi:10.1002/bit.20292, (2005).
2. Lutolf, M.P., Hubbell, J.A. Synthetic biomaterials as instructive extracellular microenvironments for morphogenesis in tissue engineering. *Nature Biotechnology.* **23**, 47-55, doi:10.1038/nbt1055, (2005).
3. Machens, H.G., Berger, A.C., Mailaender, P. Bioartificial skin. *Cells Tissues Organs.* **167**, 88-94, doi:10.1159/000016772, (2000).
4. Priya, S.G., Jungvid, H., Kumar, A. Skin tissue engineering for tissue repair and regeneration. *Tissue Engineering Part B: Reviews.* **14**, 105-118, doi:10.1089/teb.2007.0318, (2008).
5. Papavasiliou, G., Cheng, M.H., Brey, E.M. Strategies for vascularization of polymer scaffolds. *Journal of Investigative Medicine.* **58** (7), 838-844, doi:10.231/JIM.0b013e3181f18e38, (2010).

6. Laschke, M.W. *et al.* Angiogenesis in tissue engineering: breathing life into constructed tissue substitutes. *Tissue Engineering.* **12**, 2093-2104, doi:10.1089/ten.2006.12.2093, (2006).
7. Zhong, S.P., Zhang, Y.Z., Lim, C.T. Tissue scaffolds for skin wound healing and dermal reconstruction. *Wiley Interdisciplinary Reviews Nanomedicine and Nanobiotechnology.* **2** (5), 510-525, doi:10.1002/wnan.100, (2010).
8. Liu, G., Zhang, Y., Liu, B., Sun, J., Li, W., Cui, L. Bone regeneration in a canine cranial model using allogeneic adipose derived stem cells and coral scaffold. *Biomaterials.* **34** (11), 2655-64, doi:10.1016/j.biomaterials.2013.01.004, (2013).
9. Hansson, A., Di Francesco, T., Falson, F., Rousselle, P., Jordan, O., Borchard, G. Preparation and evaluation of nanoparticles for directed tissue engineering. *International Journal of Pharmaceutics.* **439** (1-2), 73-80, doi:10.1016/j.ijpharm.2012.09.053, (2012).
10. Sarkar, S.D., Farrugia, B.L., Dargaville, T.R., Dhara, S. Chitosan-collagen scaffolds with nano/microfibrous architecture for skin tissue engineering. *Journal of Biomedical Materials Research Part A.* **101**, 3482-3492, doi:10.1002/jbm.a.34660, (2013).
11. Wang, X. *et al.* The roles of knitted mesh-reinforced collagen-chitosan hybrid scaffold in the one-step repair of full-thickness skin defects in rats. *Acta Biomaterials.* **9** (8), 7822-32, doi:10.1016/j.actbio.2013.04.017, (2013).
12. Rizzi, S.C., Upton, Z., Bott, K., Dargaville, T.R. Recent advances in dermal wound healing: biomedical device approaches. *Expert Review of Medical Devices.* **1**, 143–154, doi:10.1586/erd.09.57, (2010).
13. Rieux, A. *et al.* 3D systems delivering VEGF to promote angiogenesis for tissue engineering. *Journal of Controlled Release.* **150**, 272–278, doi:10.1016/j.jconrel.2010.11.028, (2011).
14. Reckhenrich, A.K. *et al.* Bioactivation of dermal scaffolds with a non-viral copolymer-protected gene vector. *Biomaterials.* **32**, 1996-2003, doi:10.1016/j.biomaterials.2010.11.022, (2011).
15. Chen, J. *et al.* The Key Regulatory Roles of the PI3K/Akt Signaling Pathway in the Functionalities of Mesenchymal Stem Cells and Applications in Tissue Regeneration. *Tissue Engineering Part B Rev.* **19**, 516-528 (2013).
16. Fedorovich, N.E. *et al.* The role of endothelial progenitor cells in prevascularized bone tissue engineering: development of heterogenous constructs. *Tissue Engineering Part A.* **16**(7), 2355-2367 (2010).
17. Wang, L. *et al.* Osteogenesis and angiogenesis of tissue-engineered bone constructed by prevascularized β-tricalcium phosphate scaffold and mesenchymal stem cells. *Biomaterials.* **36**, 9452-9461, doi:10.1016/j.biomaterials.2010.08.036, (2010).
18. Cuadra, A. *et al.* Functional results of burned hands treated with Integra®. *Journal of Plastic, Reconstructive & Aesthetic Surgery.* **65** (2), 228-234, doi:10.1016/j.bjps.2011.09.008, (2012).
19. Wilcke, I. *et al.* VEGF(165) and bFGF protein-based therapy in a slow release system to improve angiogenesis in a bioartificial dermal substitute *in vitro* and *in vivo*. Langenbecks Arch Surg. **392** (3):305-14. Epub 2007 Apr 3, (2007).
20. Condurache, A., Aach, T., Grzybowsky S., Machens HG. Vessel segmentation and analysis in laboratory skin transplant micro-angiograms. *Proceedings of the Eighteenth IEEE Symposium on Computer-Based Medical Systems.* 21-26, doi:10.1109/CBMS.2005.104, (2005).
21. Danner, S. *et al.* The use of human sweat gland-derived stem cells for enhancing vascularization during dermal regeneration. *Journal of Investigative Dermatology.* **132** (6), 1707-16, doi:10.1038/jid.2012.31 (2012).
22. Shaterian, A. *et al.* Real Time Analysis of the Kinetics of Angiogenesis and Vascular Permeability in an Animal Model of Wound Healing. *Burns.* **35** (6), 811-7, doi: 10.1016/j.burns.2008.12.012 (2009).
23. McDonald, D.M., Choyke, P.L. Imaging of angiogenesis: from microscope to clinic. *Nature Medicine.* **9** (6), 713-725, doi:10.1038/nm0603-713, (2003).
24. Bergeron, L., Tang, M., Morris, S.F. A review of vascular injection techniques for the study of perforator flaps. *Plastic and Reconstructive Surgery.* **117**, 2050-2057, doi:10.1097/01.prs.0000218321.36450.9b, (2006).
25. Schlatter, P., König, M.F., Karlsson, L.M., Burri, P.H. Quantitative study of intussusceptive capillary growth in the chorioallantoic membrane (CAM) of the chicken embryo. *Microvascular Research.* **54** (1), 65-73, doi:10.1006/mvre.1997.2022, (1997).
26. Lehr, H.A., Leunig, M., Menger, M.D., Nolte, D., Messmer, K. Dorsal skinfold chamber technique for intravital microscopy in nude mice. *American Journal of Pathology.* **143** (4),1055-1062 (1993).
27. Menger, M.D., Jäger, S., Walter, P., Hammersen, F., Messmer, K. A novel technique for studies on the microvasculature of transplanted islets of Langerhans *in vivo*. *International journal of microcirculation, clinical and experimental.* **9** (1), 103-117 (1990).
28. Laschke, M.W. *et al.* Three-dimensional spheroids of adipose-derived mesenchymal stem cells are potent initiators of blood vessel formation in porous polyurethane scaffolds. *Acta Biomaterials.* **9** (6), 6876-84, doi:10.1016/j.actbio.2013.02.013, (2013).
29. Egaña, J.T. *et al.* Use of human mesenchymal cells to improve vascularization in a mouse model for scaffold-based dermal regeneration. *Tissue Eng Part A.* **15** (5):1191-200. doi: 10.1089/ten.tea.2008.0097, (2009).
30. Condurache, A., Aach, T. Vessel segmentation in angiograms using hysteresis thresholding. *Proceedings of the Ninth IAPR Conference on Machine Vision Applications.* 269-272 (2005).
31. Egaña, J.T. *et al.* *Ex vivo* method to visualize and quantify vascular networks in native and tissue engineered skin. *Langenbecks Archives of Surgery.* **394**, 349–356, doi:10.1007/s00423-008-0333-3, (2009).